RSC Advances

ROYAL SOCIETY OF CHEMISTRY

www.rsc.org/advances

RSC Advances

ARTICLE

Properties and Structures of β-Glucuronidases with Different Transformation Types of Glycyrrhizin

Received 00th January 20xx,
Accepted 00th January 20xx

DOI: 10.1039/x0xx00000x

www.rsc.org/

Xiaoyan Wang,[a]† Yanli Liu,[c]† Chao Wang [b], Xudong Feng [b*] and Chun Li [a,b*]

β -Glucuronidase (GUS) has been widely used to hydrolyze β-linked glucuronides to generate various valuable derivatives. In this study, the GUS from three fungi (*P*GUS from *P. purpurogenum* Li-3, *At*GUS from *A. terreus* Li-20 and *Au*GUS from *A. ustus* Li-62) with significantly different types of glycyrrhizin (GL) hydrolysis were comparatively investigated. The Km values of *P*GUS, *At*GUS and *Au*GUS were 0.328, 3.61 and 0.429 mM respectively. These results indicated that *At*GUS showed the lowest affinity for GL among the three kinds of GUS, while *P*GUS and *Au*GUS had the similar affinity for GL. Nevertheless, the Vmax / Km values displayed that *Au*GUS had the highest catalytic efficiency for GL hydrolysis, so it was supposed to be an efficient biocatalysis for GL biotransformation. The sequence properties analysis demonstrated that the three GUS had some special different sequence characteristics, but that is not the key reason for the discrepancy in catalytic type. The homologous modeling analysis indicated that various GL transformation types of *P*GUS, *At*GUS and *Au*GUS were likely caused by the different positions of bacterial loops surrounding their aglycone binding pocket. These results can not only help us to better understand the catalytic diversity of GUS, but also give us an important guide to redesign the catalytic diversity of GUS.

Introduction

β -Glucuronidase (GUS, EC 3.2.1.31) is an exoglycosidase, most of which belongs to the glycoside hydrolase family of GH2. It has been widely used in hydrolyzing β-linked glucuronides to generate their various derivatives and free glucuronic acid. The GUS also plays a role in the regulation of glucuronidation of xenobiotics and endogenous compounds, and participates in the carbohydrate metabolism in the tissues of various vertebrates.[1-6] Other extensive uses of this enzyme are as a tool for the controlled degradation of proteoglycans in structural studies and for research purposes in diagnostic and research laboratories.[7-11] The GUS has been isolated from snail, human, dog, cow, rabbit, rat and a variety of bacteria.[11,12] But so far, only few fungal species producing this enzyme have been found.

Glycyrrhizin (GL), a triterpene saponin, is the main water-soluble constituent of licorice extract (glycyrrhiza glabra). GL has been extensively used in foods, tobacco and both traditional and herbal medicine.[13,14] GL has been reported to exhibit pronounced biological activities, such as anti-cancer, anti-inflammatory, anti-bacteria, anti-oxidant and cholesterol biosynthesis inhibitory activities.[13-15] As a popular sweetener, the sweetness of GL is 170 times higher than that of sucrose.[15,16] GL is composed of one molecule of glycyrrhetinic acid (GA) and two molecules of glucuronic acid. By hydrolyzing one or two glucuronides, GL can be converted into more valuable derivatives including mono-β-glucuronide-glycyrrhizin (GAMG) and GA. GAMG not only displays higher sweetness but also shows stronger physiological functions in comparison with GL.[17-21] GA has been shown to possess several pharmacological activities advantages over GL, and it is mainly used in the pharmaceutical and cosmetic field. Presently, an efficient method is highly required to produce GAMG and GA in a large scale due to the great importance and expanding market.

It has been widely demonstrated that GUS plays a crucial role in the biotransformation of glycyrrhizin (GL) into different products.[14,22-25] To date, the GUS from human intestinal bacterium, mammal internal organ and yeast have been identified, and it is interesting that they show three different types in GL biotransformation categorized as follows: (1) GL → GAMG; (2) GL → GAMG+GA; (3) GL → GA.[15,26-29] But the reasons for these different reaction types have been rarely investigated. In this study, the mechanism will be extensively studied with focus on the structures of three GUS active domains.

Previously, three fungi (*P. purpurogenum* Li-3, *A. terreus* Li-20, and *A. ustus* Li-62) were identified in our group which could transform GL into GAMG and/or GA (Fig.1), covering all the three reaction types mentioned above.[22] In this study, the GUS from these three fungi, named *P*GUS, *At*GUS and *Au*GUS, were sequenced and characterized in vitro. Then, the transformation diversity among *P*GUS, *At*GUS and *Au*GUS was further investigated. Finally, the reasons behind different

[a] School of Chemical Engineering and Technology, State key laboratory of system bio-engineering of ministry of education, Tianjin University, Tianjin 300072, China. E-mail: xd.feng@bit.edu.cn (Xudong Feng), lichun@bit.edu.cn
[b] School of Life Science, Beijing Institute of Technology, Beijing 100081, China.
[c] School of biomedicine, Beijing city university, Beijing 100081, China.
† Authors contributed equally.

catalytic mechanism were elucidated by comparing the structure of the three GUS through modeling. This study can provide a new insight into the substrate specificity of glucuronidases towards triterpene saponins.

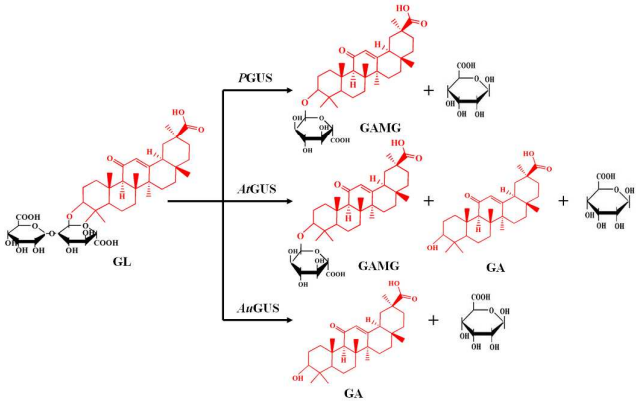

Fig. 1 Scheme of the biotransformation of GL by *P*GUS, *At*GUS and *Au*GUS.

Materials and methods

Microorganism and medium

P. purpurogenum Li-3, *A. terreus* Li-20 and *A. ustus* Li-62 were isolated and preserved by the lab of biotransformation and microecology (Beijing Institute of Technology, China).

The culture medium (1L) consisted of the following components: 3.0 g of GL, 2.2 g of KH2PO4, 3.0 g of NH4NO3, 0.05 g of Bacto-yeast extract, and 1mL of 1M MgSO4 (pH 6). All strains were incubated in shaker flasks at 30 °C and 170 rpm for 96 h.[15]

Preparation of GUS

The three strains mentioned above were inoculated into 50 mL nutrient broth in 250 mL flasks, and incubation was carried out at 170 rpm for 96 h with addition of final concentration 2 g/L of GL as substrate and inducer. After incubation of 96 h according to each optimum temperatures and pH,[22] the cells were harvested, washed and resuspended in acetate buffer (pH 4.5) for ultrasonic fragmentation in ice-water bath, and then centrifuged at 12,000 rpm for 30 min. The supernatant was first analysed with HPLC to confirm no GL was contained, and then used as a crude enzyme extract for enzymatic analysis.

Hydrolysis of glycyrrhizin

Hydrolysis types of glycyrrhizin were determined in the presence of 800 µL of 2 g/L GL (Sigma, France) as a substrate in 50 mM acetate buffer (pH 4.5) and 200 µL of the crude enzyme. The reaction mixture was incubated at 40 °C, and then terminated by boiling. After centrifugation at 10,000 rpm for 10 min, the supernatant was used to determine the amount of GL, GAMG and GA via High-performance liquid chromatography (HPLC). The analytical column was a ODS (Shim-pack, VP-ODS, Shimadzu Corporation, Kyoto, Japan, 4.6 mm×150 mm), and the UV detector was operated at 254 nm. The mobile phase was water with acetic acid / methanol (19:81, v/v, pH 2.85) with flow rate of 1 mL/min. The column chamber temperature was 40 °C, and the injection volume was 10 µL. The retention time for the standards of GL, GAMG and GA were 5.7 min, 13.7 min and 21.8 min, respectively. All determinations were performed at least twice, and the average of the values (less than 10 % deviation) was reported.

Kinetics of enzyme

The kinetics of *P*GUS, *At*GUS and *Au*GUS were determined by using GL as the substrate with concentration ranging from 0.2 to 2 g/L. Km and Vmax values were calculated by lineweaver-Burk plots using the Michaelis-Menten equation. All the experiments were carried out at 45 °C and pH 4.5. Controls without adding enzyme were made and all assays were performed in triplicate.

Total genomic DNA, RNA extraction and cDNA synthesis

The mycelia were collected through gauze filtration for extraction. Extraction of the genomic DNA was performed according to the method described by Wendland et al..[30] The total RNA was extracted with a one-step method TRIzol (Sangon, China). First-strand cDNA was synthesized using First Strand cDNA Synthesis kit (Fermentas, lithuania).

Degenerated primer design

β -glucuronidase sequences from four different fungi registered in Genbank were selected, i.e. *Penicillium canescens* (GenBank accession No. AAV91787), *Aspergillus oryzae* RIB40 (GenBank accession No. XM_001824950), *Aspergillus terreus* NIH2624 (GenBank accession No. XM_001218602), and *Aspergillus niger* (GenBank accession No. XM_001388529). After nucleotide sequence alignment, several pairs of degenerated primers were designed for the amplification of middle fragment according to the sequence identity: gusf1: 5’ -CAYTAYCCHTAYGCGGAR-3’, gusf2: 5’-GAYTTYTWYAAYTAY GCIGG-3’, gusf3: 5’-GDCTNTBGCSAAYGARCC-3’, gusd1: 5’-RA ARTCGGCRAARTTCCA-3’, gusd2: 5’-YTCNGCRTADGGRTARTG-3’, gusd3: 5’-TTSGCVANAGHCCACAT-3’, gusd4: 5’-RAARTCDGCR AARTTC-3’

Sequence analysis

ORF finder and BLAST in NCBI were used for sequence identification (http://www.ncbi.nlm.nih.gov). Phylogenetic tree was generated by Clustal X and MEGA 4.1.

Structural modeling analysis

Homologous modeling was performed by software SWISS-MODEL with the crystal structure of β- glucuronidase (PDB No. 3K46) from *E. coli* as the original model,[31] and displayed by the program PyMOL.[32] Docking between GAMG and the glucuronic acid were performed by online program AutoDock 4.2.

Results and discussions

Glycyrrhizin hydrolysis types by *P*GUS, *At*GUS and *Au*GUS

The GL hydrolysis types by the three crude enzyme extracts were investigated and the HPLC results were shown in Fig. 2. In this study, the retention time of standards samples of GL, GAMG and GA were 5.7 min, 13.7 min and 21.8 min, respectively, which were consistent with our previous publication. [33] When the conversion of GL reached around 50%, two peaks (GL 5.7 min and GAMG 13.7 min) were observed for the reaction by PGUS, and no GA was detected. When the reaction time was extended until the conversion reached above 90%, the result was still the same and no GA was formed(Supplementary File Fig. S4). All the three compounds GL, GAMG and GA were detected for the reaction by *At*GUS, while only GL and GA were shown in *Au*GUS reactants (Fig. 2). These results suggest that *P*GUS and *Au*GUS possess high chemical bond selectivity. *P*GUS can only transform GL into GAMG, without any formation of byproduct of GA. AtGUS can hydrolyze GL into two products GAMG and GA. *Au*GUS can directly transform GL into GA. The selective hydrolysis of GL by GUS from other sources has also been reported. The GUS from animal livers[34] and intestinal bacteria [35,23,36] could transform GL into both GAMG and GA. Kuramoto et al.[37] isolated a GUS from yeast *C. magnus* MG 27 which could only transform GL into GAMG. Wang et al. reported an *Aspergillus parasiticus* GUS for the conversion of GL into GA without GAMG.[38] And Park et al. also reported a GUS from bacteria *Streptococcus* LJ-22 with highly selective hydrolysis of GL into GAMG.[39] However, this is the first research about investigation of three GUS from fungi covering all the three GL hydrolysis types together.

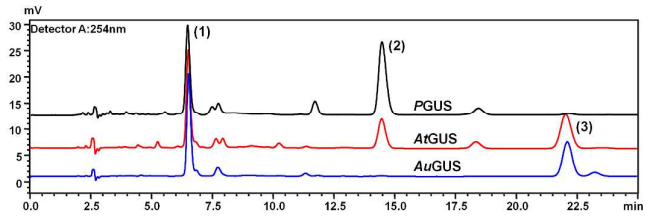

Fig. 2 The hydrolysis modes of GL catalyzed by *P*GUS (black curve), *At*GUS (red curve) and *Au*GUS (blue curve). Peak (1) was GL, Peak (2) was GAMG, and Peak (3) was GA.

Kinetics characterization

In order to get a better insight of the characteristics of *P*GUS, *At*GUS and *Au*GUS with different GL transformation modes, the kinetics of *P*GUS, *At*GUS and *Au*GUS were determined, as shown in Table 1. The apparent Km of *P*GUS, *At*GUS and *Au*GUS are 0.328, 3.61 and 0.429 mM with GL as the substrate. Km is often associated with the affinity of the enzyme for substrate,[40] so the affinity of *At*GUS for GL is the lowest among the three kinds of GUS, while *P*GUS and *Au*GUS have the similar affinity for GL. As shown in Table 2, the Vmax / Km and Vmax of *Au*GUS are twenty-three times and thirty times higher than that of *P*GUS, although it displays slightly lower affinity for GL than *P*GUS. So, *Au*GUS displays the highest catalytic efficiency for hydrolysis GL among the three kinds of GUS. Furthermore, the affinity of *At*GUS is about ten times lower than that of *P*GUS, but the Vmax is about ten times higher than that of *P*GUS. So *P*GUS and *At*GUS have almost equal catalytic efficiency for the hydrolysis GL. The variations in the affinity and the catalytic efficiency of GUS were ascribed to different species and transformation types for the same substrate. The kinetic parameters of GUS from different sources were also reported in references. Amin et al. indicated that the Km was about 1.0 mM for GUS from *Aspergillus terreus*.[14] The study by Chilke et al. showed that the Km was 2.91 mM for GUS from Indian major carp (IMC), Labeo rohita.[5]

Table 1. Kinetic parameters of the GUS from three fungi

Enzyme	K_m (mM)	V_{max} (mM min^{-1})	V_{max} / K_m (min^{-1})
*P*GUS	0.328±0.06	0.00350±0.001	0.0107±0.0020
*At*GUS	3.61±0.04	0.0340±0.005	0.00940±0.0013
*Au*GUS	0.429±0.07	0.106±0.007	0.247±0.012

Gene cloning and sequence analysis of *P*GUS, *At*GUS and *Au*GUS

Considering the significant differences in GL transformation mode and enzymatic property, the genes of *P*GUS, *At*GUS and *Au*GUS were amplified and sequenced using a genomic template for analyzing their sequence characteristic. After 5'RACE, 3'RACE and genome walking, the full encoding sequence of the three enzymes was cloned and identified (Fig. 3). The sequencing result show that the gene of *P*GUS is 1815 bp encoding 605 amino acid residues (Genbank accession No. EU095019). The 2,193 bp product of *At*GUS was amplified and its 219 bp intron was identified by NCBI (Genbank accession No. JF894133), which encodes 657 aa. And the full encoding sequence of *Au*GUS is 1824 bp with no intron (Genbank accession No. JQ897940) and encodes 608 aa. Using BLAST path as a search tool, their homologous protein sequence was searched on GenBank. The phylogenetic tree was constructed according to the BLAST results. The results showed they all had high homology to GUS from other species. The Phylogenetic analysis confirmed that the *P*GUS, *At*GUS and *Au*GUS sequences are affiliated with known GUS sequences obtained mainly from fungi (Fig. 4). Furthermore, according to *P*GUS, *At*GUS and *Au*GUS aa sequence, they have more than 69% similarity with each other (Fig. 3). And they have completely consistent sequences in several highly conserved domains. There is just one obvious difference among them that is the non-conservative sequence laid in the C-terminal. The non-conservative sequence of *At*GUS contains 65 amino acid residues, but there are only about 55 amino acid residues at the C-terminal of *P*GUS and *Au*GUS. Liu et al. verified that the non-conservative sequence of C-terminal could influence the stability and catalytic efficiency of enzyme, but had little effect on the catalytic type.[41] Therefore, structure analysis of *P*GUS, *At*GUS and *Au*GUS becomes necessary.

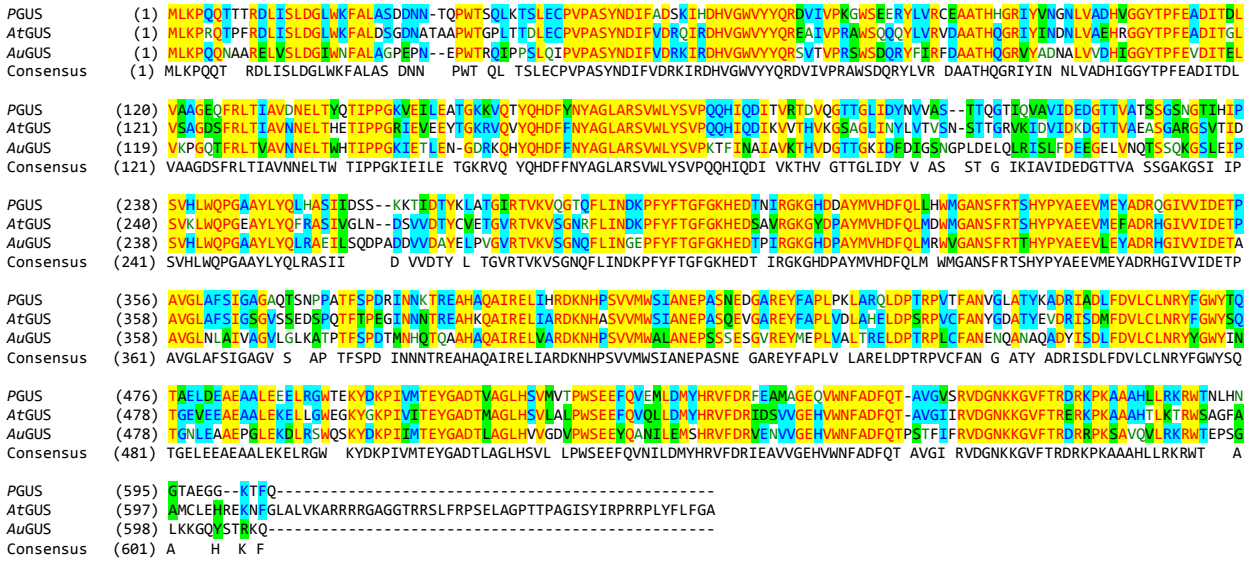

Fig. 3 Sequence alignment of *P*GUS, *At*GUS, and *Au*GUS

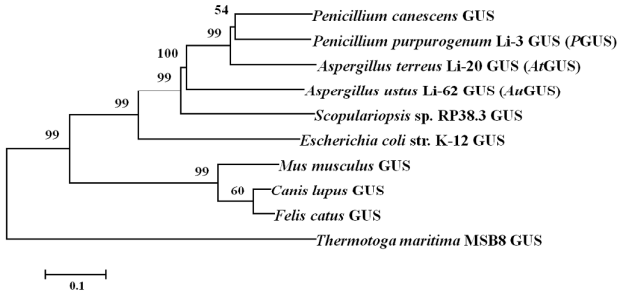

Fig. 4 Phylogenetic tree of *P*GUS, *At*GUS, and *Au*GUS with other species GUS. *Aspergillus oryzae* RIB40 GUS: XP_001825002; *Penicillium purpurogenum* GUS: ABU68712; *Penicillium canescens* GUS: AAV91787; *Aspergillus niger* CBS 513.88 GUS: XP_001388566; *Escherichia coli* K-12 GUS: AAC74689; *Mus musculus* GUS: AAA37696; *Canis lupus* GUS: AAC48809; *Chlorocebus aethiops* GUS: AAC34593; *Thermotoga maritima* MSB8 GUS: AAD36143.

Homologous modeling and substrate recognition mechanism analysis

For the structure analysis, homologous modeling was employed to analyze substrate recognition mechanism of three GUS. Using the crystal structure of β-glucuronidase (PDB No. 3K46) from *E.coli* as original model,[31] the structures of *P*GUS, *At*GUS and *Au*GUS were predicted by the online program SWISS-MODEL, and the results were analyzed with the program PyMOL (Fig. 5). All of their structures possess the typical characteristics of glycoside hydrolase family 2 (GH2 family) including three conservative domains: sugar binding domain, immunoglobulin-like beta-sandwich domain and the TIM barrel domain,[42] in which TIM barrel domain ((β/α)8 barrel domain) in the black circle was the primary catalytic domains (Fig. 5A).[43] *P*GUS, *At*GUS and *Au*GUS share most of the cartoon structure except a few loops in the results of structure-based superposition (Fig. 5A). One crucial difference is a highly flexible loop (also called bacterial loop in many articles) located on the entrance of TIM barrel domains (Fig. 5B).

The bacterial loop has also been reported to widely exist in many glycosidases, and it plays important roles in the recognition of substrates. According to previous research, the active site pockets of GH2 family are usually divided into glycosyl recognition site and aglycone binding pocket.[44] In our case, three GUS with docking GAMG and one glucuronic acid individually within the active site pocket was employed to analyze the substrate recognition mechanism. The results reveal the bacterial loop assuredly has significant influence on the recognition of substrate. As shown in Fig. 6B and C, for *At*GUS and *Au*GUS, the bacterial loop is above the aglycone binding pocket and functions as a 'lid', thus forming a tunnel-shaped substrate channel. But for *P*GUS (Fig. 6A), the bacterial loop becomes part of the aglycone binding pocket, forming a cave-shaped substrate channel. The different substrate channels may be responsible for the different GL hydrolysis modes. As mentioned above, the tunnel-shaped aglycone binding pockets of *At*GUS and *Au*GUS ensure that they can still tightly combine with substrate for the other glucuronic acid after hydrolyzing one glucuronic acid (Fig. 6B and C).[45] In addition, the aglycone binding pocket of *Au*GUS is a short and straight substrate tunnel with little steric hindrance, so the two glucuronic acid groups of GL can be consecutively hydrolyzed to form GA as the only product. While the aglycone binding pocket of *At*GUS is in the form of a snake-shaped tunnel, and it causes more steric hindrance, leading to not only the worst affinity for GL among the three GUS but also the lower enzymatic reaction rate than that of *Au*GUS, thus

forming two kinds of products GAMG and GA when hydrolyzing GL. However, the aglycone binding pocket of *P*GUS is a cave without 'lid' (Fig. 6A). This structure is likely to present an accurate space for the enzyme to bind GL with the same polar direction. After dehydrating one glucuronic acid of GL, the produced GAMG is fixed by the surrounding amino acids by polar interaction and cannot further move to glycosyl recognition site thus being released from active site pocket, resulting in GAMG as the only product. This result is similar to the substrate specificity of SbDhr1 proposed by Czjzek et al..[46-48]

Therefore, homologous modeling analysis indicates that various GL transformation modes by *P*GUS, *At*GUS and *Au*GUS are probably ascribed to the special substrate channel that were caused by the different positions of bacterial loops surrounding the aglycone binding pocket.

Conclusions

This work reports three fungi GUS: *P*GUS from *P. purpurogenum* Li-3, *At*GUS from *A. terreus* Li-20 and *Au*GUS from *A. ustus* Li-62, which have completely different reaction modes in the biotransformation of GL. The corresponding genes were cloned and identified, and phylogenetic tree indicates that they have more than 69% similarity with each other, and the obvious differences of C-terminal are not key points for catalytic type. Finally, the structural modeling analysis reveals that the various catalytic mechanisms are dependent on the different shapes of aglycone binding pocket caused by the bacterial loop. These results laid a good foundation to understand the correlation between transformational diversity of β-glucuronidases and their detailed structure.

Acknowledgements

This research was financially supported by Natural Science Foundation of China (No. 21176028, No.21425624), PhD Programs Foundation of Ministry of Education of China (No. 20121101110050) and China Postdoctoral Science Foundation (No. 2015M570038).

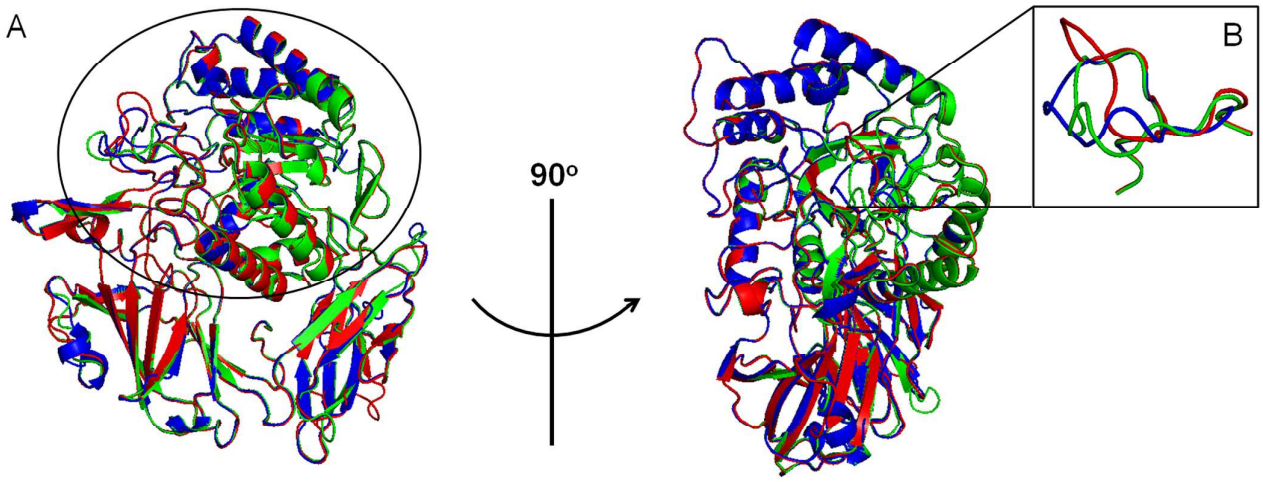

Fig. 5 Structure-based superposition of *P*GUS in green, *At*GUS in blue and *Au*GUS in red. (A) Overall structure-based superposition of *P*GUS, *At*GUS and *Au*GUS, the black circle mark the TIM barrel domain. (B) Bacterial loop structure-based superposition of *P*GUS, *At*GUS and *Au*GUS.

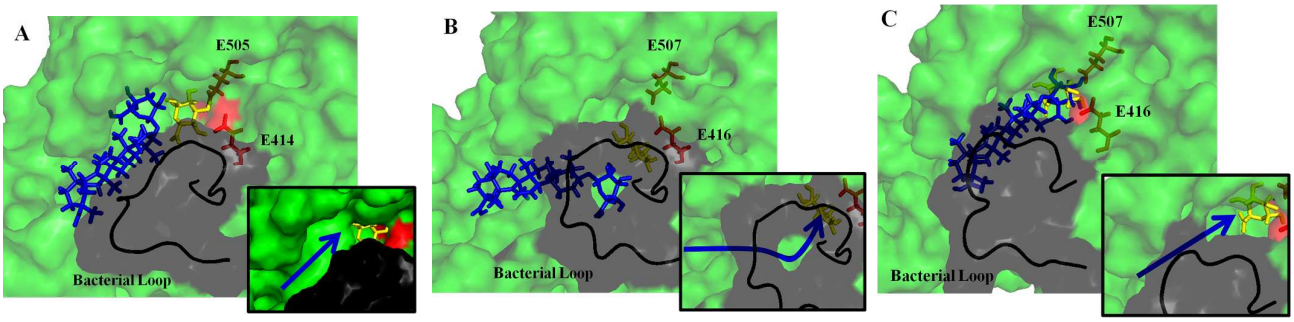

Fig. 6 Surface representation of *P*GUS, *At*GUS and *Au*GUS with docking GAMG (labeled in blue stick) and one glucuronic acid (labeled in yellow stick) within active site pocket. (A) Detailed view of *P*GUS. E414 and E505 (labeled in red stick) are two presumed activity catalytic residues. (B) Detailed view of *At*GUS. E416 and E507 (labeled in red stick) are two presumed activity catalytic residues. (C) Detailed view of *Au*GUS. E416 and E507 (labeled in red stick) are two presumed activity catalytic residues.

References

1 M.C. Gehrmann, M. Opper, H.H. Sedlacek, K. Bosslet, J. Czech, *Biochem. J.*, 1994, 301, 821-828.
2 S. Jain, W.B. Drendel, Z.W. Chen, F.S. Mathews, W.S. Sly, J.H. Grubb, *Mol. Boil.*, 1996, 4, 375-381.
3 S. Aich, T. Louis, J. Delbaere, R.D. Chen, *Protein Expres. Purif,* 2001, 22, 75-81.
4 A.M. Chilke, *Biochem*, 2010, 36, 911-915.
5 A.M. Chilke, *Biochem,* 2010, 36, 1145-1149.
6 E. Werner, C. Boursier-Neyret, B. Walther, *J. Pharmaceut Biomed*, 2010, 53, 1070-1073.
7 B. Thomasset, M. Menard, H. Boetti, L.A. Denmat, D. Inzke, D. Thomasa, *Plant Sci,* 1996, 113, 209-219.
8 H. Kuroyama, N. Tsutsui, Y. Hashimoto, Y. Tsumuraya, *Carbohydr. Res*, 2001, 333, 27-39.
9 B. Sperker, T.E. Murdter, J.T. Backman, P. Fritz, H.K. Kroemer, *Life Sci*, 2002, 71, 1547-1557.
10 M.J. Callanan, W.M. Russell, T.R. Klaenhammer, Gene, 2007, 389, 122-127.
11 R. Chouiter, I. Roy, C. Bucke, *J. Mol. Catal. B: Enzym*, 2008, 50, 114-120.
12 M. Mroczynska, Z. Libudzisz, *J. Microbiol*, 2010, 59, 265-269.
13 T. Akao, *Biol. Pharm. Bull,* 1999, 22, 80-82.
14 H.A. Amin, H.A. El-Menoufy, A.A. El-Mehalawy, Mostafa ES, *J. Mol. Catal. B: Enzym*, 2011, 69, 54-59.
15 S.J. Feng, C. Li, X.L. Xu, X.Y Wang, *J. Mol. Catal, B: Enzym*, 2006, 43, 63-67.
16 S.J. Feng, C. Li, Z.A. Cao, *Chinese Journal of Bioprocess Engineering*, 2006, 4, 16-21.
17 J.H. Zhou, Y.D. Cui, B.N. Li, H.R. Yang, *Food Additive. Chemical industry Beijing,* 2001, 170-172.
18 Z.K. Song, X.Y. Wang, G.Q. Chen, C. Li, *Journal of Chemical Industry and Engineering*, 2008, 59, 3101-3106.
19 S. Farese, A. Kruse, A. Pasch, Dick B, M.B. Frey, D.E. Uehlinger, F.J. Frey, *Kidney Int*, 2009, 76, 877-884.
20 P. Kalaiarasi, K.V. *Pugalendi, Eur. J. Pharmacol*, 2009, 606, 269-273.
21 B.D. Wallace, H.W. Wang, K.T. Lane, *J.E Scott, Science*, 2010, 330, 831-836.
22 C. Wang, X.X. Guo, X.Y. Wang, F. Qi, S.J. Feng, C. Li, *World J Microbiol Biotechnol*, 2013, 29, 781–788.
23 T. Akao, *Biol. Pharm. Bull*, 2000, 23, 6-11.
24 D. Nurizzo, T. Nagy, H.J. Gilbert, G.J. Davies, *Structure*, 2002, 10, 547-556.
25 Y. Hu, L. Yang, S.L. Yang, *Pharm.Biotechnol*, 2006, 13, 66-70.
26 W.H. Fishman, *J. Biol. Chem*, 1991, 127, 367.
27 H.S. Yu, S.J. Wu, F.X. Jin, Y. Guo, *Food and Fermentation Industries*, 1998, 25, 10-15.
28 H.S. Yu, S.J. Wu, F.X. Jin, Y. Guo, *Food and Fermentation Industries*, 1999, 25, 5-12.
29 S.J. Wu, Z.J. Yang, L.H. Zhu, F.X. Jin, *Chinese Traditional and Herbal Drugs*, 2003, 34, 516-519.
30 J. Wendland, K. B. Lengeler, E. Kothe, *Fungal Genet Newslett*, 1996, 43, 54–55.
31 B.D. Wallace, H. Wang, K.T. Lane, J.E. Scott, J. Orans, J.S. Koo, M. Venkatesh, C. Jobin, L.A. Yeh, S. Mani, M.R. Redinbo, *Science*, 2010, 330 (6005), 831-835.
32 W.L. DeLano, *Palo Alto. CA. DeLano Scientific*, 2002.
33 S.P. Zou, G.Y. Liu, I. Kaleem, C. Li, *Process Biochemistry*, 2013, 48, 358-363.
34 T. Akao, M. Hattori, M. Kanaoka, K. Yamamoto, T. Namba, K. Kobashi, *Biochem Pharmacol*, 1991, 41, 1025-1034.
35 D.H. Kim, K. Lee, K. Han, *Biol Pharm Bull*, 1999, 23, 320-322.
36 T. Akao, *Biol Pharm Bull*, 2001, 24, 1108–1120.
37 T. Kuramoto, Y. Ito, M. Oda, Y. Tamura, S. Kitahara, *Biosci Biotechnol Biochem*, 1994, 58, 455–463.
38 J. Wang, Q. Sun, P. Gao, J.F. Wang, C. Xu, Q.L. Sun, *Appl Microbiol Biotechnol*, 2010, 46, 421–426.
39 H.Y. Park, N.Y. Kim, M.J. Han, E.A. Bae, D.H. Kim, *J microbiol Biotechnol*, 2005, 15, 792–801.
40 P.C Engel, *Enzyme kineytics: the steady-state approach*, *London: Chapman and hall*, 1977, 14.
41 Y.L. Liu, J. Huangfu, F. Qi, I. Kaleem, W.W. E, C. Li, *PloS one*, 2012, 7, e30998.
42 S. Jain, W.B. Drendel, Z.W. Chen, *Nat Struct Biol*, 1996, 3, 375-381.
43 B. Höcker, C. Jürgens, M. Wilmanns, *Curr Opin Biotechnol*, 2001, 12, 376-381.
44 S. Tribolo1, J.G. Berrin, P.A. Kroon, M. Czjzek, N. Juge, *J. Mol. Biol*, 2007, 370, 964-975.
45 D. Nurizzo, T. Nagy, J. Gilbert, G.J. Davies, *Structure*, 2002, 10, 547-556.
46 M. Czjzek, M. Cicek, V. Zamboni, *Proc Natl Acad Sci*, 2000, 97, 13555-13560.
47 M. Czjzek, M. Cicek, V. Zamboni, *Biochem J*, 2001, 354, 37-46.
48 L. Verdoucq, J. Moriniere, D.R. Bevan, *J Biol Chem*, 2004, 279, 31796-31803.

